metals

MDPI

Article

Elasto-Plastic Behaviour of Transversely Isotropic Cellular Materials with Inner Gas Pressure

Zhimin Xu [1], Kangpei Meng [2], Chengxing Yang [2], Weixu Zhang [1,*], Xueling Fan [1] and Yongle Sun [2,*]

[1] State Key Laboratory for Strength and Vibration of Mechanical Structures, School of Aerospace Engineering, Xi'an Jiaotong University, Xi'an 710049, China

[2] School of Mechanical, Aerospace and Civil Engineering, The University of Manchester, Sackville Street, Manchester M13 9PL, UK

* Correspondence: zhangwx@mail.xjtu.edu.cn (W.Z.); yongle.sun@manchester.ac.uk (Y.S.); Tel.: +86-029-82668-754 (W.Z.); +44-016-1275-1916 (Y.S.)

Received: 7 July 2019; Accepted: 14 August 2019; Published: 16 August 2019

Abstract: The fabrication process of cellular materials, such as foaming, usually leads to cells elongated in one direction, but equiaxed in a plane normal to that direction. This study is aimed at understanding the elasto-plastic behaviour of transversely isotropic cellular materials with inner gas pressure. An idealised ellipsoidal-cell face-centred-cubic foam that is filled with gas was generated and modelled to obtain the uniaxial stress–strain relationship, Poisson's ratio and multiaxial yield surface. The effects of the elongation ratio and gas pressure on the elasto-plastic properties for a relative density of 0.5 were investigated. It was found that an increase in the elongation ratio caused increases in both the elastic modulus and yield stress for uniaxial loading along the cell elongation direction, and led to a tilted multiaxial yield surface in the mean stress and Mises equivalent stress plane. Compared to isotropic spheroidal-cell foams, the size of the yield surface of the ellipsoidal-cell foam is smaller for high-stress triaxiality, but larger for low-stress triaxiality, and the yield surface rotates counter-clockwise with the Lode angle increasing. The gas pressure caused asymmetry of the uniaxial stress–strain curve (e.g., reduced tensile yield stress), and it increased the nominal plastic Poisson's ratio for compression, but had the opposite effect for tension. Furthermore, the gas pressure shifted the yield surface towards the negative mean stress axis with a distance equal to the gas pressure. The combined effects of the elongation ratio and gas pressure are complicated, particularly for the elasto-plastic properties in the plane in which the cells are equiaxed.

Keywords: foam; enclosed gas; anisotropy; elasticity; plasticity; multiaxial yielding

1. Introduction

Cellular materials, either natural or manmade, are unique with regard to mechanical, thermal, acoustic and electromagnetic properties, benefitting from their high porosity, which reduces the overall density, enhances the energy absorption capacity and enables the integration of multiple functions. Foams, made of metals, polymers, ceramics, etc., are typical cellular materials, and they are widely used in transport, aerospace, defence, building and biomedical industries [1,2].

In the fabrication of foams, the cell structure is determined by the foaming process, which is sensitive to the foaming agent used and the state of the base material during the foaming [3]. It is common that the cell structure is anisotropic after fabrication, particularly when gravity plays an important role in the foaming process. Foams usually consist of cells which are elongated in one direction, but equiaxed in the plane perpendicular to the elongation direction, exhibiting transversely isotropic structural characteristics [4]. However, most previous studies focused on the elasto-plastic

behaviour of presumably isotropic foams [5–8], and there is still a paucity of experimental and modelling data for better understanding the anisotropic elasto-plastic behaviour of foams. Therefore, more studies on anisotropic foams are needed for both uniaxial and multiaxial loadings, which are pertinent to applications of foams as energy absorbers and cores of sandwich structures.

Closed-cell foams contain inner trapped gas in the cells after fabrication and the inner gas pressure can considerably affect the macroscopic elasto-plastic properties [1]. It is also of fundamental significance and scientific interest to study the effect of gas pressure on the elasto-plastic behaviour of closed-cell foams. For static loading, Ozgur et al. [9] analysed the effect of gas pressure on the elastic properties of cellular materials using 2D finite element (FE) models, in which hexagonal, rectangular and circular cells were considered. Öchsner and Mishuris [10] developed a 3D simple cubic cell model and numerically analysed the gas effects on the stress–strain relationship, Poisson's ratio, Young's modulus and yield surface. Zhang et al. [11] established a theoretical model using second-order moment of stress with consideration of inner gas pressure, and they overcame the limitation of an earlier theoretic model [12] and clarified the gas effect. Based on the Gurson yield function [13], Guo et al. [14–17] developed a thick-walled spherical unit cell model and systematically studied the yield behaviour of metal foams with inner gas pressure. For dynamic loading, Sun and Li [18] investigated the effects of gas pressure on the dynamic strength and deformation of cellular materials, and their findings have been applied to explain experimental observations on dynamic compressive behaviour of closed-cell foams [2]. However, these previous studies all focused on isotropic cellular materials. There is still a lack of modelling studies on the elasto-plastic behaviour of anisotropic cellular materials with inner gas pressure.

In this study, an idealised transversely isotropic cellular material with inner gas pressure, i.e., gas-filled ellipsoidal-cell face-centred-cubic (FCC) foam, is studied numerically. The ellipsoidal cell is elongated in one direction, but equiaxed in the plane normal to the elongation direction. Different elongation ratios are considered to investigate the effects of anisotropy on static elasto-plastic properties (e.g., uniaxial stress–strain relationship, Poisson's ratio and multiaxial yield surface). The effects of gas pressure on the anisotropic elasto-plastic properties are also investigated.

2. Material and Methods

The typical cell structure of a transversely isotropic closed-cell foam is shown in Figure 1a, along with the inner gas pressure. To facilitate modelling without losing key physics, one representative volume (RV) unit is considered, as shown in Figure 1b. The RV simplification of geometry implies that the cells are periodically arranged in 3D space, as well as cell deformation, in contrast to the random distribution of irregular cells and cell deformation in an actual closed-cell foam that is normally seen. Nevertheless, provided that the closed-cell foam possesses transversely isotropic macro-properties, a mechanical model based on RV geometry is deemed reliable to capture qualitative behaviour and gain general insights. The enhanced computational efficiency obtained by the geometric simplification enables the analysis of sufficient loading cases in modelling to investigate both the uniaxial and multiaxial elasto-plastic behaviour of the closed-cell foam. A similar RV approach has been widely used for the analysis of the elasto-plastic behaviour of cellular materials [10,19,20].

The RV unit is idealised to be an FCC unit with ellipsoidal cells, as shown in Figure 1b. The ellipsoid is elongated in the y direction (Figure 1c) and mathematically described as

$$\frac{(x^2+z^2)}{{a_1}^2}+\frac{y^2}{{a_2}^2}\le 1 \tag{1}$$

where a_1 and a_2 are the axial radii in the isotropic plane (i.e., x-z plane) and along the elongation direction (i.e., y direction), respectively. The elongation ratio is thus defined as $R = a_2/a_1$.

The relative density of a cellular material is

$$f = \rho/\rho_s \tag{2}$$

where ρ and ρ_s are the densities of the cellular material and the base material, respectively. For the closed-cell FCC foam, the relative density can also be determined from geometric parameters, viz.

$$f = 1 - \frac{16\pi {a_1}^2 a_2}{3L^3} \tag{3}$$

Here, L is the size of the cubic unit, which is kept constant. We adopted $f = 0.5$ in this study. It should be noted that, for given R, L, and f, the values of a_1 and a_2 can be uniquely determined.

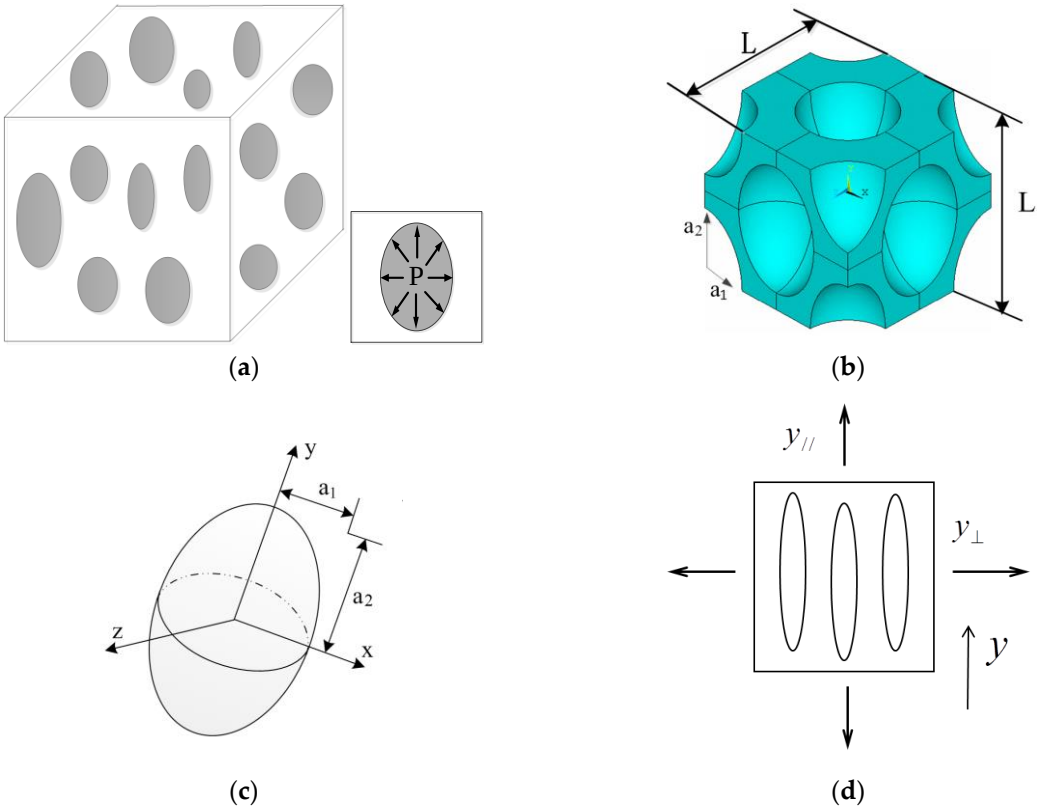

Figure 1. (**a**) Typical cell structure of transversely isotropic closed-cell foam with inner gas pressure; (**b**) representative volume (RV) unit of ellipsoidal-cell face-centred-cubic (FCC) foam; (**c**) orientation of the ellipsoidal cell, which is equiaxed in the x-z plane, but elongated in the y direction; (**d**) definition of directions parallel and perpendicular to the elongation direction (i.e., y-direction).

The multiaxial plastic behaviour of cellular materials is complicated. It has been demonstrated that the yield surface of an isotropic foam is dependent on both the first and second stress invariants [2,6]. For transversely isotropic cellular materials, the yield surface may be more complicated and the locus of yield points may not be unique if only the first and second stress invariants are used in characterisation. Therefore, a full description of the stress state should be provided. In general, three parameters are needed to determine each point in the principal stress space, and here, the mean stress, Mises equivalent stress and Lode angle are adopted. It should be noted that these stress parameters are solely associated with the type of loading and are independent of the constitutive behaviour of the material which is either isotropic or not isotropic. The mean stress is expressed as

$$\sigma_m = \frac{\sigma_{kk}}{3} \tag{4}$$

with Einstein's summation convention applied. The familiar Mises equivalent stress is given by

$$\sigma_e = \sqrt{3J_2} = \sqrt{\frac{3}{2} s_{ij} s_{ij}} \tag{5}$$

where J_2 is the second deviatoric stress invariant, and s_{ij} is the deviatoric stress, i.e., $s_{ij} = \sigma_{ij} - \sigma_m \delta_{ij}$, ($i$, j = 1, 2, 3). The stress triaxiality is thus obtained via

$$X_\Sigma = \frac{\sigma_m}{\sigma_e} \tag{6}$$

The Lode angle is defined as follows:

$$L = -\cos(3\theta) = -\left(3\frac{\sqrt[3]{\frac{1}{2}J_3}}{\sigma_e}\right)^3 = -\frac{27}{2}\frac{J_3}{\sigma_e^3} = -\frac{27}{2}\frac{Det(s_{ij})}{\sigma_e^3} \tag{7}$$

where L is the Lode parameter, θ is the Lode angle and J_3 is the third deviatoric stress invariant.

It is assumed that the principal stress direction coincides with the axial direction of the ellipsoidal cell, i.e., $\sigma_1 = \sigma_{11}$, $\sigma_2 = \sigma_{22}$ and $\sigma_3 = \sigma_{33}$. Accordingly, the relationship between the principal stress, mean stress, Mises equivalent stress and Lode angle is given as follows:

$$\frac{3}{2\sigma_e}\{\sigma_1, \sigma_2, \sigma_3\} = \left\{-\cos\left(\theta + \frac{\pi}{3}\right), -\cos\left(\theta - \frac{\pi}{3}\right), \cos\theta\right\} + \frac{3}{2\Sigma}\{1,\ 1,\ 1\} \tag{8}$$

In the ellipsoidal-cell FCC foam model, only one eighth of the RV unit is considered (Figure 2a) owing to symmetry. Multiaxial loading is applied according to Equation (8), as shown in Figure 2b, where T_1, T_2 and T_3 are axial loads in three principal directions. Any state of loading stress can be obtained by varying the ratio of the three axial loads.

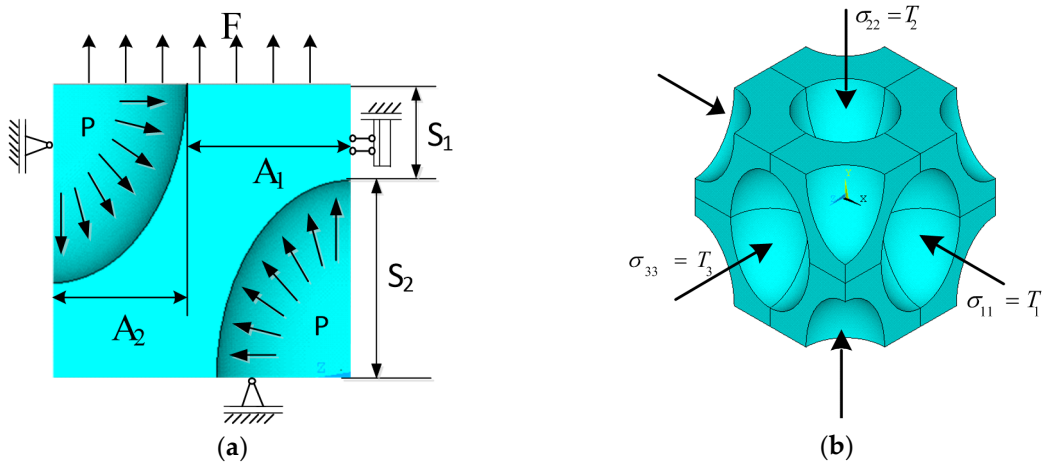

Figure 2. (**a**) Schematic of ellipsoidal-cell face-centred-cubic (FCC) foam model (only 1/8 volume is considered owing to symmetry); (**b**) application of multiaxial loading.

Details of the loading process are described below:

1) Inner gas pressure is applied and meanwhile, an additional load is applied to balance the inner gas pressure. Note that the gas pressure refers to the gauge pressure after the subtraction of ambient air pressure. Öchsner and Mishuris [10] concluded that the inner gas pressure only causes slight deformation and thus the gas pressure is assumed to be constant throughout the loading process. Taking a uniaxial loading case as an example, the area A_1 of the solid in Figure 2a is on the loading boundary, where a balancing load to the inner gas pressure P needs to be applied, in addition to the main load. The equilibrium equation is given as

$$\int_{A_2} P\mathrm{d}A_2 = -\int_{A_1} F'\mathrm{d}A_1 \tag{9}$$

where A_1 and A_2 are the areas of the solid and gas, respectively, as shown in Figure 2a. F' denotes the balancing load to the inner gas pressure P. The method for balancing gas pressure is the same when applying loads in other directions;

2) The relationship between triaxial loads and invariant stress parameters has been given in Equation (8). Accordingly, the loads to be applied in the three axial directions are calculated and determined for different stress states. This provides guidance on the application of multiaxial loads to maximise the attainable stress states in the principal stress space, and the multiaxial loading is applied in a proportional manner;

3) The macroscopic stress and strain is calculated. Taking uniaxial loading as an example, the macroscopic stress can be calculated using the following formula:

$$\overline{\sigma} = \frac{1}{A_1 + A_2}\left(\int_{A_1} F\mathrm{d}A_1 + \int_{A_2} P\mathrm{d}A_2 + \int_{A_1} F'\mathrm{d}A_1\right) \tag{10}$$

where F is the main load applied to the FCC foam. Taking into account Equation (9), the macroscopic stress can be expressed as

$$\overline{\sigma} = \frac{1}{A_1 + A_2}\int_{A_1} F\mathrm{d}A_1 \tag{11}$$

The corresponding macroscopic strain $\overline{\varepsilon}$ can be expressed as

$$\overline{\varepsilon} = \overline{\varepsilon}_F - \overline{\varepsilon}_P - \overline{\varepsilon}_{F'} \tag{12}$$

where $\overline{\varepsilon}_F$, $\overline{\varepsilon}_P$ and $\overline{\varepsilon}_{F'}$ are the strains corresponding to the main load F, inner gas pressure P and the balancing load F' to the gas pressure, respectively. Similarly, macroscopic stresses and strains in other directions can be obtained. Finally, the macroscopic Mises equivalent stress and equivalent strain can be calculated via

$$\overline{\sigma}_e = \sqrt{\frac{3}{2}\overline{S}_{ij}\overline{S}_{ij}} \tag{13}$$

$$\overline{\varepsilon}_e = \sqrt{\frac{2}{3}\overline{e}_{ij}\overline{e}_{ij}} \tag{14}$$

where $\overline{S}_{ij}$ and $\overline{e}_{ij}$ are the macroscopic deviatoric stress and strain tensors, respectively.

General purpose FE software ANSYS® was employed in numerical modelling. Linear solid elements (ANSYS designation SOLID185) were used and the FE mesh consisted of 61,091 elements, as shown in Figure 3. A mesh sensitivity analysis was performed, which showed that the numerical results of stress and strain were unchanged when further refining the mesh.

It is assumed that the base material conforms to Hooke's elasticity law and von Mises plasticity theory, i.e.,

$$\sigma = \begin{cases} E_s\varepsilon, & \text{for } \varepsilon \le \varepsilon_0 \\ \sigma_s + E_p(\varepsilon - \varepsilon_0), & \text{for } \varepsilon > \varepsilon_0 \end{cases} \tag{15}$$

where E_s and E_p are the elastic modulus and plastic hardening modulus, respectively; σ_s and ε_0 are the initial yield stress and yield strain, respectively. For a qualitative study on cellular materials in general, the following parameters are assumed: E_s = 3.5 GPa, E_p = 0.1 GPa, σ_s = 80 MPa and Poisson's ratio = 0.33.

The initial yield stress of the ellipsoidal-cell FCC foam is defined as the intersection of the extrapolated linear elastic portion and plastic portion in the macroscopic stress–strain curve, as proposed by Deshpande and Fleck [21]. For multiaxial loading, the Mises equivalent stress–strain curve and mean stress–strain curve are used to determine the initial yield surface. The Poisson's ratio of

the ellipsoidal-cell FCC foam is defined as the absolute value of the ratio of macroscopic strains perpendicular and parallel to the loading direction, respectively.

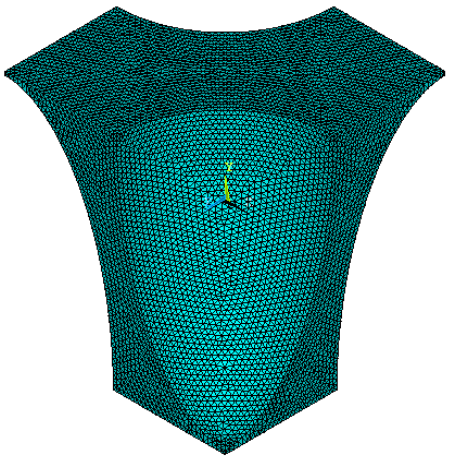

Figure 3. Finite element (FE) mesh of ellipsoidal-cell face-centred-cubic (FCC) foam model (only 1/8 volume is considered owing to symmetry).

3. Results and Discussion

3.1. Uniaxial Stress-Strain Relationship

Figure 4 shows the uniaxial stress–strain curves of the FCC foam loaded along the ellipsoidal-cell elongation direction, when different values of gas pressure and elongation ratio are considered. For a typical elongation ratio (R = 2), increasing the gas pressure does not change the linear elastic portion of the stress–strain curve, but the plastic portion is significantly affected, as shown in Figure 4a. Without inner gas pressure, the stress–strain curve is antisymmetric between tension and compression, but such anti-symmetry is violated by the presence of gas pressure. When the gas pressure increases, the tensile yield stress markedly decreases, while the compressive yield stress only slightly decreases (in magnitude). For spheroidal-cell foam, Xu et al. [20] found a similar effect of gas pressure on tensile yield stress, but a slight increase in compressive yield stress due to gas pressure, in contrast to the observation in Figure 4a. It is surmised that the gas pressure can exacerbate the deformation concentration at the end of the long axis when compressive load is applied along the long axis, thereby promoting macroscopic yielding at a lower stress level for the ellipsoidal-cell foam, compared to the compressive behaviour of spheroidal-cell foam [20]. Nevertheless, for both spheroidal-cell and ellipsoidal-cell foams, the effect of gas pressure on the uniaxial stress–strain curve is more pronounced in tension than in compression.

Figure 4b shows the uniaxial stress–strain curves of the gas-filled ellipsoidal-cell FCC foam with different elongation ratios. For a given value of gas pressure (P = 15 MPa), increasing the elongation ratio leads to an increase in yield stress for both tension and compression, to a lesser extent for the latter. The elastic modulus (i.e., slope of the linear elastic portion) also increases. The above observation demonstrates a strong effect of the elongation ratio on the uniaxial elasto-plastic behaviour of the gas-filled FCC foam loaded along the cell elongation direction. The increases in both yield stress and elastic modulus can be attributed to the fact that a higher elongation ratio implies more material is distributed to bear the load applied in the cell elongation direction.

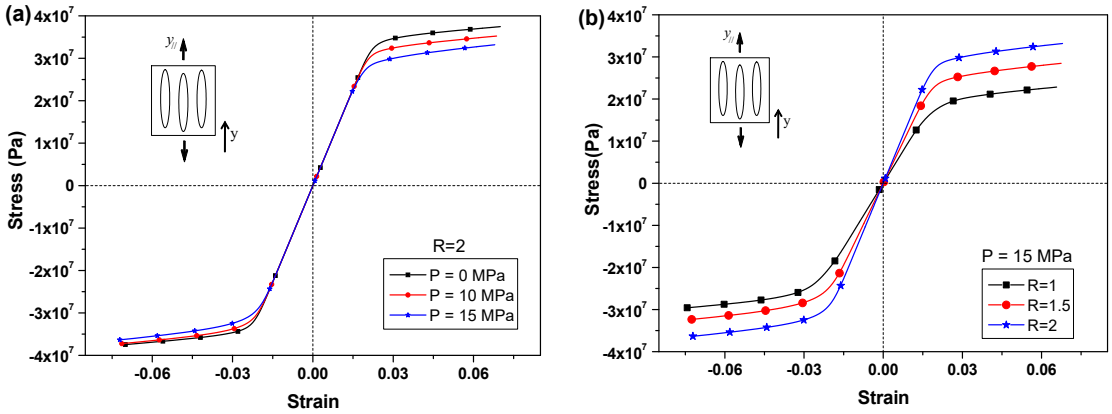

Figure 4. Uniaxial stress–strain curves of the ellipsoidal-cell face-centred-cubic (FCC) foam loaded along the cell elongation direction for different values of inner gas pressure (**a**) and elongation ratio (**b**).

Figure 5 shows the uniaxial stress–strain curves of the FCC foam when the loading direction is perpendicular to the cell elongation direction. Figure 5a shows the gas effect when the elongation ratio is two. Again, the gas pressure hardly affects the elastic modulus and the effect of gas pressure on the tensile stress–strain curve is similar to that in the parallel loading case (Figure 4a). However, the gas pressure enhances the magnitude of compressive yield stress, unlike the decreasing trend found in the parallel loading case (Figure 4a). It is expected that the gas pressure can contribute to an enhanced resistance of the FCC foam to compressive load, since the gas pressure can be directly additive to the compressive load-bearing capacity, except that undesirable deformation potentially induced by gas pressure could cause an adverse effect (e.g., slight decrease in compressive yield stress, as observed in Figure 4a). Figure 5b shows the effect of the elongation ratio on the uniaxial stress–strain curve of the gas-filled ellipsoidal-cell FCC foam. It appears that increasing the elongation ratio does not affect the elastic modulus, but causes a reduction in tensile yield stress, in contrast to the increasing trend found in the parallel coating case (Figure 4b). The effect of the elongation ratio on the compressive yield stress is similar between the perpendicular and parallel loading cases.

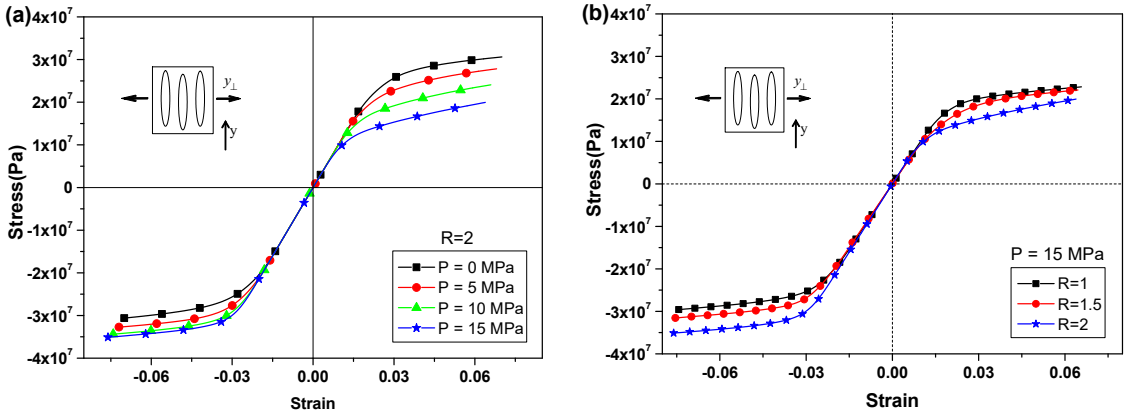

Figure 5. Uniaxial stress–strain curves of the ellipsoidal-cell face-centred-cubic (FCC) foam loaded perpendicularly to the cell elongation direction for different values of inner gas pressure (**a**) and elongation ratio (**b**).

Comparing the results shown in Figures 4 and 5, one can conclude that (1) given an elongation ratio greater than one, the elastic modulus and tensile yield stress are larger in the long axial direction than in the short axial direction, whether inner gas pressure is present or not; however, the compressive yield stress is affected by gas pressure in opposite ways between the parallel loading and perpendicular loading, although when gas pressure is absent, the compressive yield stress is higher in the long axial direction than in the short axial direction; (2) given the gas pressure, the elongation ratio plays a more

significant role in the uniaxial elasto-plastic behaviour under parallel loading than under perpendicular loading; (3) in general, the gas pressure hardly affects the elastic modulus, and it has less effect on the uniaxial plastic behaviour under parallel loading than under perpendicular loading.

3.2. Poisson's Ratio

Figure 6a,b shows the Poisson's ratio of the FCC foam uniaxially loaded parallelly and perpendicularly to, respectively, the cell elongation direction. It should be noted that the Poisson's ratio of isotropic spheroidal-cell foam ($R = 1$) is independent of the loading direction. By contrast, for ellipsoidal-cell foam, the Poisson's ratio does not vary in the equiaxed-cell plane (x-z plane) for the parallel loading (Figure 6a), but it differs between the long and short axes for the perpendicular loading (Figure 6b). The prominent feature is that when the gas pressure is absent, the Poisson's ratio is symmetric between tension and compression and such symmetry is independent of the elongation ratio and loading direction. When the elongation ratio increases, the Poisson's ratio becomes larger in the parallel loading case (Figure 6a), but smaller in the perpendicular loading case (Figure 6b). The gas pressure does not affect the Poisson's ratio in the elastic stage, but its effect is significant in the plastic stage, wherein the gas pressure decreases the Poisson's ratio for tension, but increases the Poisson's ratio for compression. As a result, the Poisson's ratio becomes asymmetrical between tension and compression. The effect of gas pressure on Poisson's ratio can be explained as follows. For uniaxial tension, the gas pressure and tensile loading are aligned, which favours the deformation along the loading direction and thus reduces the Poisson's ratio. Conversely, the gas pressure counteracts the compressive load and thereby increases the Poisson's ratio under uniaxial compression. Such trends hold for different elongation ratios. A similar gas effect on Poisson's ratio was also reported by Xu et al. [20] and Öchsner and Mishuris [10] for isotropic cellular materials.

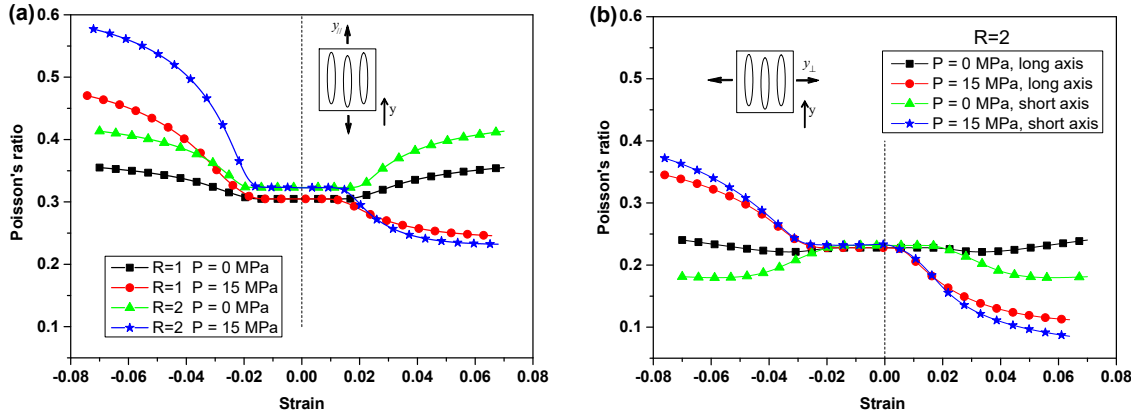

Figure 6. Poisson's ratio of the ellipsoidal-cell face-centred-cubic (FCC) foam loaded parallelly (**a**) and perpendicularly to (**b**) the cell elongation direction. Note that for perpendicular loading, the Poisson's ratio differs between the short and long axes.

3.3. Multiaxial Yield Surface

Figure 7 shows the initial yield surfaces of the FCC foam under multiaxial loading at different Lode angles. For a Lode angle of 0°, when the elongation ratio is one (i.e., spheroidal-cell foam) and the gas pressure is zero, the yield surface is an ellipse, being symmetrical about the σ_e axis in the $\sigma_e - \sigma_m$ plane, but such symmetry is violated when the elongation ratio is two, leading to a yield surface manifested as a tilted ellipse in the $\sigma_e - \sigma_m$ plane. It is clearly seen that the yield surface of the transversely isotropic ellipsoidal-cell FCC foam is distinct from the yield surface of the isotropic spheroidal-cell FCC foam. Particularly, compared to the spheroidal-cell foam, the ellipsoidal-cell foam is more susceptible to yielding when approaching a hydrostatic stress state (i.e., yield stress is lower when $X_\Sigma \to \infty$), but it is more resistant to yielding when approaching a shear stress state (i.e., yield stress is higher when $X_\Sigma \to 0$). The Lode angle does not affect the yield surface of the spheroidal-cell

foam ($R = 1$), but it does affect the orientation of the tilted yield surface of the ellipsoidal-cell foam ($R = 2$), i.e., the yield surface rotates counter-clockwise when the Lode angle is increasing.

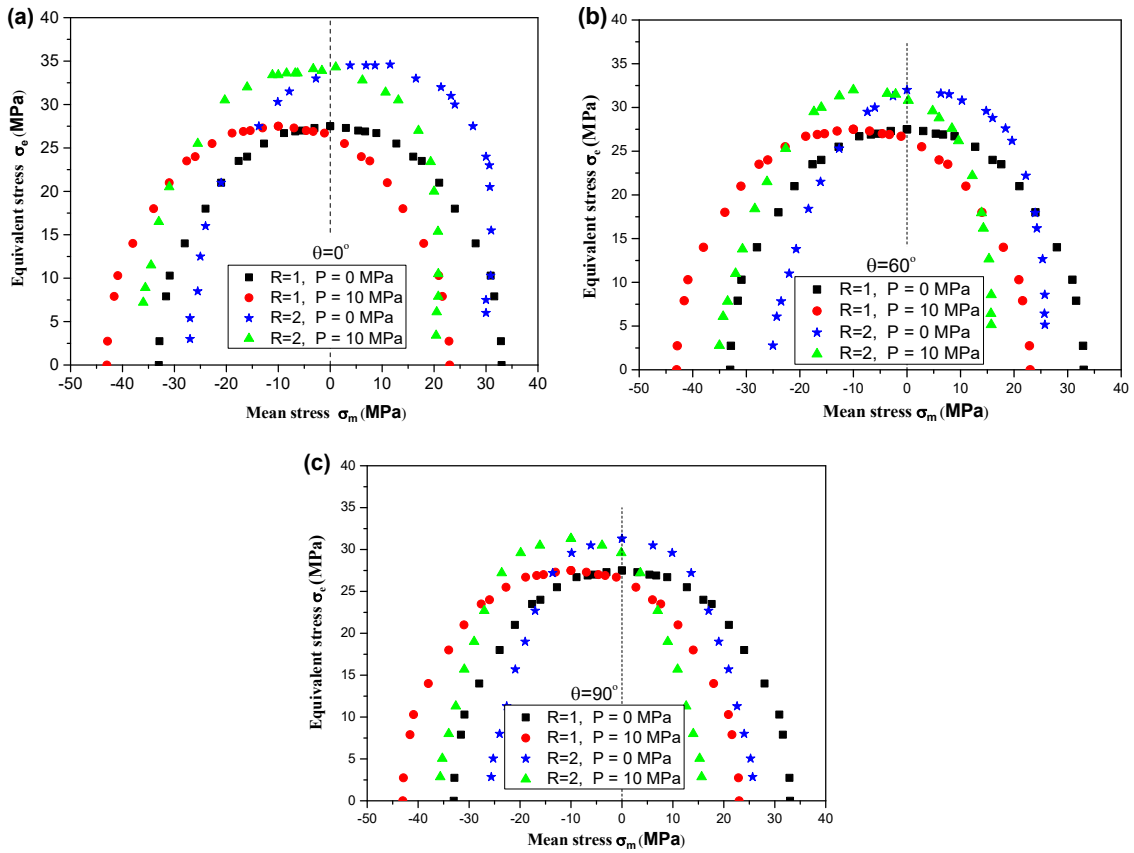

Figure 7. Initial multiaxial yield surfaces of the ellipsoidal-cell face-centred-cubic (FCC) foam for Lode angles of 0° (**a**), 60° (**b**) and 90° (**c**).

The effect of gas pressure on the yield surface is straightforward, i.e., the gas pressure shifts the yield surface towards the negative mean stress axis with a distance equal to the gas pressure in the $\sigma_e - \sigma_m$ plane. Such an effect is independent of the Lode angle and elongation ratio, which is consistent with the previous studies by Xu et al. [20] and Zhang et al. [11].

4. Conclusions

A qualitative study on the elasto-plastic properties of transversely isotropic cellular materials with inner gas pressure is presented, which is focused on a gas-filled ellipsoidal-cell FCC foam with a relative density of 0.5. The findings are summarised as follows:

(1) The elasto-plastic behaviour of the gas-filled ellipsoidal-cell FCC foam is dependent on the loading direction. The effect of the elongation ratio is most pronounced for uniaxial loading along the cell elongation direction. Increasing the elongation ratio leads to increases in the elastic modulus, yield stress and Poisson's ratio, due to more load-bearing material being distributed in the elongation direction. For perpendicular loading, increasing the elongation ratio does not affect the elastic modulus, but reduces the tensile yield stress and Poisson's ratio, and increases the compressive yield stress. In general, the elastic modulus, tensile yield stress and Poisson's ratio are higher for parallel loading than for perpendicular loading. For multiaxial loading, the initial yield surface of the ellipsoidal-cell FCC foam is a tilted ellipse in the $\sigma_e - \sigma_m$ plane and it rotates counter-clockwise when the Lode angle is increasing;

(2) The inner gas pressure causes asymmetry of the uniaxial stress–strain curve of the FCC foam. It reduces the tensile yield stress, but it has the opposite effects on the compressive yield stress for

loadings parallel and perpendicular to the cell elongation direction, i.e., slight reduction for the former, while a considerable increase for the latter. The effect of gas pressure on the uniaxial stress–strain curve is more pronounced in tension than in compression. Poisson's ratio is independent of gas pressure in the elastic regime, but it increases in the plastic compression regime and decreases in the plastic tension regime, due to the effect of gas pressure. Furthermore, the gas pressure shifts the tilted multiaxial yield surface of the ellipsoidal-cell foam towards the negative mean stress axis with a stress value identical to the gas pressure value.

Author Contributions: Conceptualization, W.Z. and Y.S.; methodology, Z.X. and X.F.; software, Z.X. and X.F.; validation, K.M. and C.Y.; formal analysis, Z.X. and Y.S.; investigation, Z.X., K.M. and C.Y.; resources, W.Z., X.F. and Y.S.; data curation, K.M. and C.Y.; writing—original draft preparation, Z.X. and Y.S.; writing—review and editing, K.M., C.Y., X.F. and W.Z.; visualization, Z.X.; supervision, W.Z.; project administration, X.F.; funding acquisition, W.Z. and Y.S.

Funding: This research was funded by the China State Key Laboratory for Strength and Vibration of Mechanical Structures through Open Project (grant number SV2018-KF-37) and the National Natural Science Foundation of China (grant numbers 11772246, 11472203, 11172227, U1530259).

Acknowledgments: The authors are grateful to Fulin Shang at XJTU for insightful discussion.

Conflicts of Interest: The authors declare no conflict of interest.

References

1. Gibson, L.J.; Ashby, M.F. *Cellular Solids: Structure and Properties*, 2nd ed.; Cambridge University Press: Cambridge, UK, 1997.
2. Sun, Y.; Li, Q.M. Dynamic compressive behaviour of cellular materials: A review of phenomenon, mechanism and modelling. *Int. J. Impact Eng.* **2018**, *112*, 74–115. [CrossRef]
3. Banhart, J. Manufacture, characterisation and application of cellular metals and metal foams. *Prog. Mater. Sci.* **2001**, *46*, 559–632. [CrossRef]
4. Huber, A.T.; Gibson, L.J. Anisotropy of foams. *J. Mater. Sci.* **1988**, *23*, 3031–3040. [CrossRef]
5. Sun, Y.; Amirrasouli, B.; Razavi, S.B.; Li, Q.M.; Lowe, T.; Withers, P.J. The variation in elastic modulus throughout the compression of foam materials. *Acta Mater.* **2016**, *110*, 161–174. [CrossRef]
6. Deshpande, V.S.; Fleck, N.A. Isotropic constitutive models for metallic foams. *J. Mech. Phys. Solids* **2000**, *48*, 1253–1283. [CrossRef]
7. Abrate, S. Criteria for yielding or failure of cellular materials. *J. Sandw. Struct. Mater.* **2008**, *10*, 5–51. [CrossRef]
8. Zhang, W.X.; Wang, T.J. Effect of surface energy on the yield strength of nanoporous materials. *Appl. Phys. Lett.* **2007**, *90*, 063104. [CrossRef]
9. Ozgur, M.; Mullen, R.L.; Welsch, G. Analysis of closed cell metal composites. *Acta Mater.* **1996**, *44*, 2115–2126. [CrossRef]
10. Öchsner, A.; Mishuris, G. Modelling of the multiaxial elasto-plastic behaviour of porous metals with internal gas pressure. *Finite Elem. Anal. Des.* **2009**, *45*, 104–112. [CrossRef]
11. Zhang, W.; Xu, Z.; Wang, T.J.; Chen, X. Effect of inner gas pressure on the elastoplastic behavior of porous materials: A second-order moment micromechanics model. *Int. J. Plast.* **2009**, *25*, 1231–1252. [CrossRef]
12. Kitazono, K.; Sato, E.; Kuribayashi, K. Application of mean-field approximation to elastic-plastic behavior for closed-cell metal foams. *Acta Mater.* **2003**, *51*, 4823–4836. [CrossRef]
13. Gurson, A.L. Continuum Theory of Ductile Rupture by Void Nucleation and Growth: Part I—Yield Criteria and Flow Rules for Porous Ductile Media. *J. Eng. Mater. Technol.* **1977**, *99*, 2–15. [CrossRef]
14. Guo, T.F.; Cheng, L. Modeling vapor pressure effects on void rupture and crack growth resistance. *Acta Mater.* **2002**, *50*, 3487–3500. [CrossRef]
15. Guo, T.F.; Cheng, L. Vapor pressure and void size effects on failure of a constrained ductile film. *J. Mech. Phys. Solids* **2003**, *51*, 993–1014. [CrossRef]
16. Cheng, L.; Guo, T.F. Void interaction and coalescence in polymeric materials. *Int. J. Solids Struct.* **2007**, *44*, 1787–1808. [CrossRef]
17. Guo, T.F.; Faleskog, J.; Shih, C.F. Continuum modeling of a porous solid with pressure-sensitive dilatant matrix. *J. Mech. Phys. Solids* **2008**, *56*, 2188–2212. [CrossRef]

18. Sun, Y.; Li, Q.M. Effect of entrapped gas on the dynamic compressive behaviour of cellular solids. *Int. J. Solids Struct.* **2015**, *63*, 50–67. [CrossRef]
19. McElwain, D.L.S.; Roberts, A.P.; Wilkins, A.H. Yield criterion of porous materials subjected to complex stress states. *Acta Mater.* **2006**, *54*, 1995–2002. [CrossRef]
20. Xu, Z.M.; Zhang, W.X.; Wang, T.J. Deformation of closed-cell foams incorporating the effect of inner gas pressure. *Int. J. Appl. Mech.* **2010**, *02*, 489–513. [CrossRef]
21. Deshpande, V.S.; Fleck, N.A. Multi-axial yield behaviour of polymer foams. *Acta Mater.* **2001**, *49*, 1859–1866. [CrossRef]